5th ECPMG Delft · 2024

Proceedings of the 5th ECPMG 2024
5th European Conference on Physical Modelling in Geotechnics
2-4 October 2024, Delft, the Netherlands

Dynamic centrifuge modelling of the seismic deformation response in level ground and its evaluation

Dong-Chao Zhang, Yan-Guo Zhou*, Zheng-Bo Sun, Yun-Min Chen
*MOE Key Laboratory of Soft Soil and Geoenvironmental Engineering, Institute of Geotechnical Engineering, Center for Hypergravity Experiment and Interdisciplinary Research, Zhejiang University, Hangzhou, P. R. China. *E-mail: qzking@zju.edu.cn*

ABSTRACT: The earthquake-induced deformation response of the level ground could be classified into two types: Type A, observed for non-liquefaction events, and Type B, observed after liquefaction triggering. Reliable evaluation of dynamic and post-earthquake deformations of grounds under condition of Type A is crucial for the performance-based design of foundations and geotechnical infrastructures. In this study, a series of cyclic triaxial tests were conducted to establish a correlation between the safety factor of liquefaction and the peak excess pore pressure ratio of saturated sand. An empirical model for residual excess pore pressure is also proposed to evaluate the degradation of shear modulus and compression modulus of soil elements, which are subsequently utilized to estimate the dynamic shear strain during shaking and the post-earthquake volumetric strain. Consequently, the dynamic deformation and post-earthquake settlement of a level ground could be evaluated by the safety factor of liquefaction. Then a dynamic centrifuge model test of saturated level ground was conducted and the deformation response of the model ground was carefully observed. By comparing the predicted deformations with the observations in the model test, the applicability of the proposed method was preliminarily validated.

1 INTRODUCTION

Earthquake-induced ground deformation directly threaten the safety of foundations and geotechnical infrastructures. Some efforts have been made in evaluating the post-liquefaction deformation of ground (e.g., Zhou et al., 2023), while the evaluation of seismic deformation of ground before liquefaction triggering urges a reliable estimation of excess pore pressure generation and the corresponding reduction of the shear modulus and compression modulus (Karamitros et al., 2013).

Many stress-based excess pore pressure models (e.g., Park et al., 2015, Chiaradonna et al., 2018) have been proposed. However, most of them either underestimate the excess pore pressure ratios (r_u) at low r_u, where r_u is defined as the ratio of excess pore pressure to overburden effective stress. In this study, we conducted a series of undrained triaxial shear tests on loose sand and proposed an empirical pore pressure model characterized by the liquefaction safety factor (FS_{liq}). By utilizing this model, we predicted the pore pressure response in a level centrifuge model ground during dynamic shaking. Additionally, we considered the attenuation curve of the shear modulus of the sand and the re-consolidation compression curve to predict the maximum shear strain of the foundation induced by earthquake and post-seismic settlement. These predictions served as preliminary validation of the accuracy of our proposed empirical pore pressure model and seismic deformation evaluation method.

2 LIQUEFACTION SAFETY FACTOR BASED -DYNAMIC DEFORMATION EVALUATION METHOD

2.1 Liquefaction Safety Factor-Based Pore Pressure Generation Model

Based on the *CRR*(*N*) relationship proposed by Idriss & Boulanger (2008), Chiaradonna and Flora (2020) proposed a simple expression of the safety factor FS_{liq} as shown in Equation (1).

$$\mathrm{FS}_{\mathrm{liq}} = \left(\frac{N}{N_{\mathrm{L}}}\right)^{-b} \tag{1}$$

where the CRR is the cyclic resistance ratio, which equals to the cyclic shear stress ratio (CSR) required to reach liquefaction in a specified number of loading cycles (N); N_L is the number of loading cycles required for liquefaction triggering of saturated sand in a specified CSR. The parameter b is a fitting parameter.

By combining the characteristics of excess pore pressure generation pattern in saturated sand under cyclic loading, a segmented fitting function is proposed as follows:

$$r_{\mathrm{u}}=\begin{cases}0.5\cdot FS_{liq}^{\alpha}\,(r_{\mathrm{u}}\le \mathrm{r_{u,ref}})\\ \frac{2}{\pi}\arcsin\left(FS_{liq}{}^{-\frac{1}{b}}\right)^{\frac{1}{2\beta}}\,(r_{\mathrm{u}}>\mathrm{r_{u,ref}})\end{cases}\quad(2)$$

where $r_{\mathrm{u,ref}}$ is the reference residual excess pore pressure ratio which represents the initial anisotropy of soil has been totally damaged by cyclic loadings. The $r_{\mathrm{u,ref}}$ is influenced by many parameters (e.g. relative density (D_{r}) and cyclic shear stress (CSR)), with its overall range falling between 0.4 and 0.7. The parameter α and β are fitting parameters.

It should be noted that once $r_{\mathrm{u,ref}}$ and the corresponding $\mathrm{FS}|_{ru=ru,\mathrm{ref}}$ are determined, the fitting parameter β could be directly calculated. Therefore, the above equation only requires determination of one fitting parameter α.

2.2 Cyclic triaxial liquefaction tests

In this study, a series of cyclic triaxial liquefaction tests were conducted on the saturated Fujian sand with 10% Qiantang river silt (abbreviated as FS-10 bellow) to obtain the liquefaction strength of the sands and the generation process of pore pressure ratio. The gravity density is G_{s}=2.647 g/cm^3, and the maximum and minimum dry density are $\rho_{\mathrm{d,max}}$=1.765 and $\rho_{\mathrm{d,min}}$=1.386. More exhausted information could be found in Zhou et al. (2021). The relative density of soil is 50%, and all the tests were under the same confining pressure of 100 kPa. The frequency of cyclic loading was 0.05 Hz.

Fig. 1 presents the liquefaction strength fitted by a power function. The fitting parameters b in Eq. (1) is -0.118.

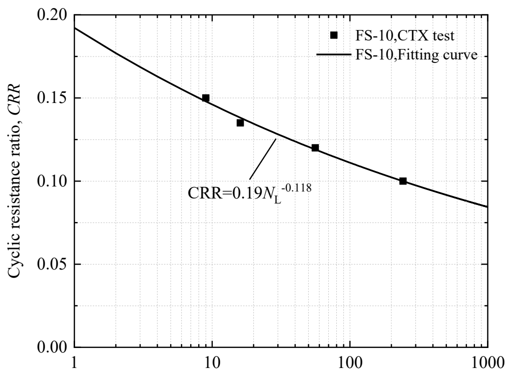

Figure 1. Cyclic liquefaction resistance curve for FS-10(σ'_m=100 kPa).

Based on the Eq. (1), the relationship between the residual excess pore pressure ratio r_{u} and the cycle ratio N/N_{L} are transformed into the r_{u}-$\mathrm{FS_{liq}}$ relationship as shown in Fig. 2. It should be noted that the r_{u} here is normalized by the maximum residual excess pore pressure ratio $r_{\mathrm{u,max}}$. For the loose FS-10 sand, the $r_{\mathrm{u,ref}}$ = 0.4 is selected here because of the optimal fitting performance for all the curves.

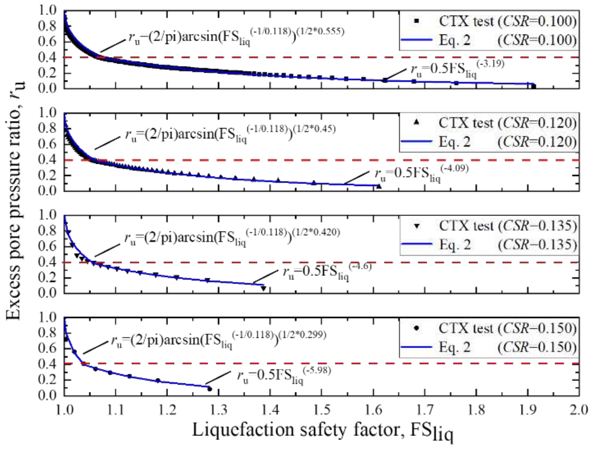

Figure 2. The fitting curves of r_u-FS_{liq} relationship under different cyclic shear stress ratio.

2.3 Estimation of maximum shear strain and reconsolidation volumetric strain

For the dry sand or saturated sand without considerable generation of excess pore pressure, the degradation of shear modulus with shear strain could be described by the Ramberg-Osgood equation as follows:

$$\gamma=\frac{\tau_c}{G_0}\cdot\left[1+\left(\frac{2}{\gamma_{\mathrm{ref}}}\cdot\frac{\tau_c}{G_0}\right)^{\theta-1}\right],\theta=\frac{2+\pi\cdot h_{max}}{2-\pi\cdot h_{max}}\quad(3)$$

where G_0 is the small-strain secant shear modulus, $h_{\max}$ is the maximum damping ratio, and γ_{rf} is the reference shear strain value at which G/G_0=0.5.

The G_0 here is 84 MPa under the confining pressure of 100 kPa. The corresponding $\square_{\mathrm{ref}}$ and θ are 0.041% and 2.47, respectively. Once the maximum excess pore pressure ratio is determined, according to Hardin equation (Hardin and Blandford, 1989), the G_0 could be replaced by $G_0(1\text{-}r_{\mathrm{u}})^{\mathrm{n}}$ where n is the fitting parameter in Hardin equation and n=0.43 for FS-10.

Fig.3 presents the relationship between the reconsolidation compression modulus and the excess pore pressure ratio obtained from the undrained cyclic triaxial test. As r_{u} and $E_{\mathrm{s}}(r_{\mathrm{u}})$ could be determined with reference to Fig. 2 and Fig. 3, the reconsolidation volumetric strain after shaking could be readily calculated as follows:

$$\varepsilon_{\mathrm{v,r}}=\frac{\sigma_v'}{E_s(r_u)}=\frac{\sigma_v(1-r_u)}{E_s(r_u)}\quad(4)$$

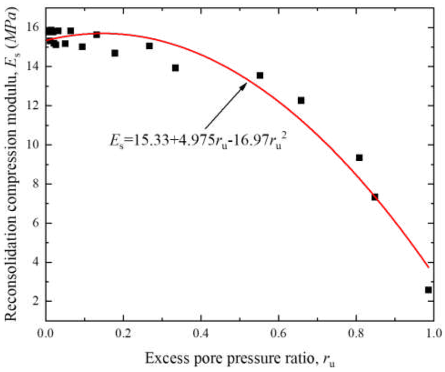

Figure 3. The reconsolidation compression curve of FS-10 with D_r=50%.

3 DYNAMIC CENTRIFUGE MODELLING OF THE SEISMIC DEFORMATION RESPONSE IN LEVEL GROUND

3.1 Model configuration

To explore the applicability of the aboved method in predicting the seismic deformation response, a dynamic centrifuge model test of the level ground of the same soil with the same relative density is conducted.

The model ground was prepared using air-pluviation method with a target void ratio e_0=0.705 (i.e., D_r=50%). The model ground was saturated by vacuum method. The model configuration is shown in Fig. 4. After spin up to the designated centrifugal acceleration of 50 g, a prototype scale 1 Hz sine wave of peak amplutidue of 0.08 g consisting of fifteen constant amplitude cycles with additional three smaller ramped cycles at the beginning and the end, was chosen as the input motion.

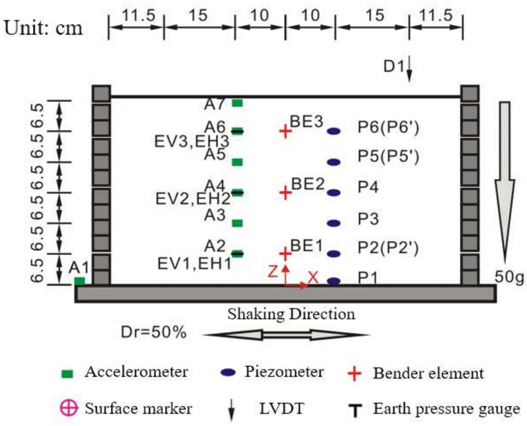

Figure 4. The model configuration (geometry in model scale).

3.2 Validation of the FS$_{liq}$-based seismic deformation evaluation method

Based on the acceleration time histories shown in Fig. 5 (a), the cyclic shear stress ratio (*CSR*) of model ground at different depths could be calculated by the following equation (see Fig. 5 (b)):

$$CSR = \frac{\tau_{av}}{\sigma_v'} = \frac{\sum_{i=1}^{n}(\rho_i \Delta h_i a_{\max,i}(z))}{\sigma_v'} \tag{5}$$

where the τ_{av} is the equivent seismic shear stress;σ'_v is the vertical stress at certain depth of the model; h_i is the depth of soil between each accelerator;a_{max} is the maximum acceleration at each depth.

The maximum shear strain at each depth could be determined by the second-order interpolation between displacements at different depths, which could be integrated by recorded accelerations. The calculation method based on accelerometer array in ground could be bereferred in Zeghal et al. (2018).

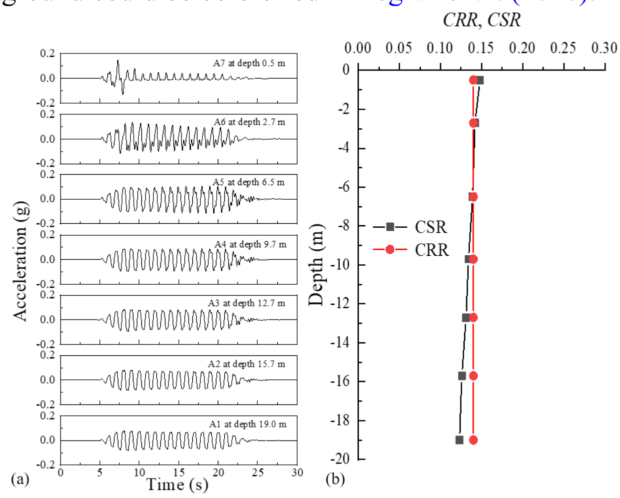

Figure 5. Model test result: (a) The acceleration time history and (b) CSR at different depths of model ground.

Fig. 6 exhibits the comparision of the predicted and recorded excess pore pressure ratioat each depth. The empirical pore pressure model proposed in this study performs well in predicting the pore pressure development trend of non-liquefied conditions. However, it tends to underestimate the pore pressure development of surface soils which undergos larger *CSR*. Further improvements are needed in this regard. Nevertheless, the prediction accuracy of the peak excess pore pressure ratio preliminarily verified the applicability of the proposed method.

Finally, the shaking-induced maximum cyclic shear strain at different depths could be calculated using Eq. (3), and the comparion with the recorded value is given in Fig. 7(a). The post-shaking settlement could be calculated using Eq. (4), and the comparion with the recorded value is given in Fig. 7(b).

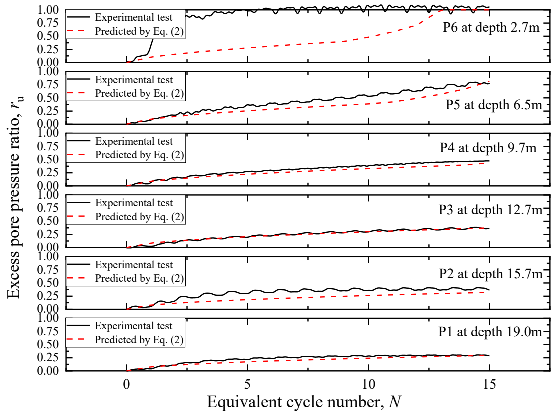

Figure 6. Comparison between the predicted and recorded excess pore pressure ratio at different depths.

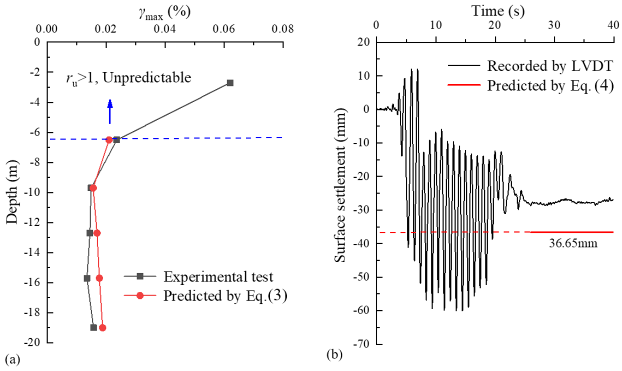

Figure 7. Comparison between the predicted and recorded values: (a) maximum cyclic shear strain at different depth and (b) the post-earthquake settlement.

4 CONCLUSIONS

This paper proposed a new evaluation method of excess pore pressure ratio generation based on the safety factor of soil liquefaction, and the degradation of shear modulus and compression modulus of soil are determined by considering the generation of excess pore pressure. Therefore, the seismic deformation response could be approximately predicted by the safety factor of soil liquefaction, which provides a promising way in engineering practices.

The applicability of the proposed method is preliminarily validated by a centrifuge model test of a level ground. However, for other conditions, such as different relative densities and earthquake motion intensities, the proposed method requires further investigation and validation.

ACKNOWLEDGEMENTS

This study is supported by the National Natural Science Foundation of China (Nos. 51988101, 51978613, 52278374) and the Chinese Program of Introducing Talents of Discipline to University (the 111 Project, B18047).

REFERENCES

Chiaradonna, A., Tropeano, G., d'Onofrio, A., Silvestri, F. (2018) Development of a simplified model for pore water pressure build-up induced by cyclic loading. *Bulletin of Earthquake Engineering*.;16. https://doi.org/10.1007/s10518-018-0354-4

Chiaradonna, A., Flora, A. (2020) On the estimate of seismically induced pore-water pressure increments before liquefaction. *Géotechnique Letters*;10(2):128-34. https://doi.org/10.1680/jgele.19.00032

Hardin, B. O., and Blandford, G. E. 1989. Elasticity of particulate materials. *Journal of Geotechnical Engineering*, 115(6): 788-805.https://doi.org/10.1061/(ASCE)07339410(1989)115:6(788)

Idriss, I. M., and Boulanger, R. W. (2008). Soil liquefaction duringearthquakes, Monograph MNO-12. Oakland, CA, USA: *Earthquake Engineering Research Institute*.

Karamitros, D. K., Bouckovalas, G. D., Chaloulos, K. I. and Adrianopoulos, K. I. (2013). Numerical analysis of liquefaction-induced bearing capacity degradation of shallow foundations on a two-layered soil profile. *Soil Dyn. Earthq. Engng* 44, 90 – 101.https://doi.org/10.1016/j.soildyn.2012.07.028

Park T, Park D, Ahn J. K. (2015). Pore pressure model based on accumulated stress. *Bull EarthqEng*13(7):1913–1926.https://doi.org/10.1007/s10518-014-9702-1

Zhou Y-G, Zhang D-C, Liu K, Chen Y-M. (2024) Post-liquefaction deformation mechanisms of stone column-improved liquefiable sloping ground under cyclic loadings. *Soil Dynamics and Earthquake Engineering*;177:108340.https://doi.org/10.1016/j.soildyn.2023.108340

Zhou Y-G, Liu K, Sun Z-B, Chen Y-M. (2021) Liquefaction mitigation mechanisms of stone column-improved ground by dynamic centrifuge model tests. Soil Dynamics and Earthquake Engineering;150:106946.https://doi.org/10.1016/j.soildyn.2021.106946

Zeghal M, Goswami N, Kutter BL, Manzari MT, Abdoun T, Arduino P, et al. (2018) Stress-strain response of the LEAP-2015 centrifuge tests and numerical predictions. Soil Dynamics and Earthquake Engineering;113:80418.https://doi.org/10.1016/j.soildyn.2017.10.014